

Received November 10, 2019, accepted November 24, 2019, date of publication November 27, 2019, date of current version December 12, 2019.

Digital Object Identifier 10.1109/ACCESS.2019.2956214

NFC-Enabled Far-Field Antenna on PET Flexible Substrate for 3G/4G/LTE Mobile Devices

BANCHA LUADANG¹, (Member, IEEE),
ARNON SAKONKANAPONG², (Student Member, IEEE),
SITTHICHAJ DENTRI³, (Member, IEEE), **RASSAMITUT PANSOMBOON**⁴, (Member, IEEE),
AND CHUWONG PHONGCHAROENPANICH², (Member, IEEE)

¹Department of Instrumentation Engineering, Faculty of Engineering, Rajamangala University of Technology Rattanakosin, Nakhon Pathom 73170, Thailand

²Department of Telecommunications Engineering, Faculty of Engineering, King Mongkut's Institute of Technology Ladkrabang, Bangkok 10520, Thailand

³College of Industrial Technology, King Mongkut's University of Technology North Bangkok, Bangkok 10800, Thailand

⁴Wireless and Intelligent System for Dual-Use Application Research Division, National Security and Dual-Use Center, National Science and Technology Development Agency, Pathumthani 12120, Thailand

Corresponding author: Bancha Luadang (bancha.lua@rmutr.ac.th)

This work was supported by the Institute of Research and Development, Rajamangala University of Technology Rattanakosin.

ABSTRACT This research presents a far-field (FF) antenna with near-field communication (NFC) capability for 3G/4G/LTE mobile devices. The integrated far- and near-field communication (FNFC) antenna was fabricated using conductive silver ink on polyethylene terephthalate (PET) flexible substrate. The FF segment of the antenna is operable in the frequency range of 1.8-2.1 GHz, and the NFC antenna is of dual loop and operable at 13.56 MHz. In the antenna realization, simulations were performed and, to validate, an antenna prototype was fabricated. The experimental results revealed that the FF antenna achieved an impedance bandwidth of 37% (1.52-2.21 GHz), given $|S_{11}|$ of less than -6 dB, with the minimum and maximum efficiency of 92.1% and 98%. The experimental gains are 1.76-2.08 dBi across the target operating frequency band, with near-omnidirectional radiation pattern. The simulation and experimental results are in good agreement. Moreover, the FNFC antenna achieves strong magnetic field distributions in H_x , H_y , and H_z orientations and holds promising potential for 3G/4G/LTE applications.

INDEX TERMS Conductive ink antenna, flexible substrate antenna, integrated antenna, mobile antenna.

I. INTRODUCTION

Flexible electronics technologies play an important role in the development of modern wireless smart devices. Of particular interest is flexible printed electronics on thin films, papers, textiles, and a variety of flexible substrates. The aim is to mass-produce electronics components that are lightweight, lean, shapeable, durable, and economical [1]–[3].

Specifically, flexible antennas have been deployed in wireless local area network (2.45/5.2/5.8 GHz) and 3G/4G applications (1.8/1.9/2.1 GHz) [4]–[6]. These antennas however are restricted to far-field functions for WLAN and 3G/4G applications, rendering it less suitable for modern wireless communication devices in which both near-field and far-field communication functions are required.

Furthermore, a double exponentially tapered slot antenna (DE TSA) on flexible liquid crystal polymer organic material

was proposed for UWB applications [7]. Meanwhile, a multilayer dual-frequency (14 and 35 GHz) dual-polarization microstrip array antenna on liquid crystal polymer was developed for Ku and millimeter-wave applications [8]. In [9], the researchers designed a microstrip patch antenna on flexible polymer (SU-8/PMDS). In [10], a novel class of conformal antennas based on embroidered conductive fibers on polymer substrates was proposed. In addition, antennas based on Kapton polyimide substrate, which is known for its flexibility, robustness, and thermal endurance, were proposed for WLAN and Bluetooth applications [11]. The usefulness of these antennas is limited to far-field applications, however. Attempts have thus been made to improve the performance of printed flexible antennas based on copper, silver, or conductive polymers [12]–[16].

The planar inverted F antenna (PIFA) structure is commonly used in sensor networks and mobile clients in wireless communication systems [17]. In [18]–[20], inkjet-printing PIFA antennas based on organic substrate were employed

The associate editor coordinating the review of this manuscript and approving it for publication was Abhishek Kandwal¹.

to economize the manufacturing cost. However, these antennas lack the near-field communication (NFC) function (i.e., restricted to far-field function).

With the advent of cashless economy and changes in consumer behavior, NFC technology in the smart device becomes increasingly important. NFC is a short-range wireless communication technology operating at 13.56 MHz with low power consumption. The communication distance is approximately 10 cm with a maximum data transfer rate of 424 kbit/s. To enable NFC capability in a smart phone or a tablet, users only need to tap or touch an NFC reader or device with the mobile device.

This research presents an integrated FNFC (far- and near-field communication) antenna based on PIFA structure for 3G/4G/LTE applications. The FNFC antenna is operable at 1.8-2.1 GHz and was fabricated using conductive silver ink on polyethylene terephthalate (PET) flexible substrate. Simulations were carried out using CST Microwave Studio Suite [21] for optimal parameters of the integrated FNFC antenna. An antenna prototype was subsequently fabricated and experiments undertaken.

The organization of this research is as follows: Section I is the introduction. Section II details the antenna design, consisting of the far-field and near-field segments of the antenna; and surface current distribution and magnetic field distribution analysis. Section III discusses the fabrication of prototype antenna and experimental results. The concluding remarks are provided in Section IV.

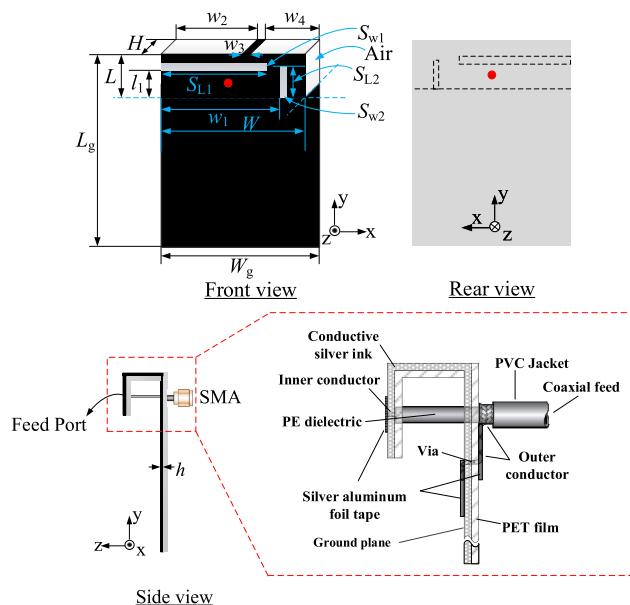


FIGURE 1. Configuration of the far-field segment of integrated FNFC antenna.

II. ANTENNA DESIGN

A. FAR-FIELD ANTENNA

Figure 1 illustrates the far-field (FF) segment of the antenna based on PIFA structure, following [22] with minor modifications. The FF antenna consists of two conductor layers: the

TABLE 1. Characteristic parameters of the substrate and conductive silver ink.

Materials	Characteristics	Value
Polyethylene terephthalate (PET substrate)	Thickness	100 μm
	Relative permittivity	3.5
	Loss tangent	0.002
Conductive silver ink (HPS-012LV)	Electrical conductivity	1.6×10^6 S/m
	Ag content	75%
	Specific gravity	3.1

TABLE 2. The optimal design parameters of FF segment of the antenna.

Parameters	Description	Physical size (mm)	Electrical size		
			1.8 GHz	1.9 GHz	2.1 GHz
L	The length of patch	10	$0.06 \lambda_1$	$0.06 \lambda_2$	$0.07 \lambda_3$
W	The width of patch	40	$0.24 \lambda_1$	$0.25 \lambda_2$	$0.28 \lambda_3$
L_g	The length of ground plane	50	$0.30 \lambda_1$	$0.32 \lambda_2$	$0.35 \lambda_3$
W_g	The width of ground plane	40	$0.24 \lambda_1$	$0.25 \lambda_2$	$0.28 \lambda_3$
H	The distance between patch and ground plane	8.0	$0.05 \lambda_1$	$0.05 \lambda_2$	$0.06 \lambda_3$
SL_1	The length of slit_1	30	$0.18 \lambda_1$	$0.19 \lambda_2$	$0.21 \lambda_3$
SW_1	The width of slit_1	1.2	$0.007 \lambda_1$	$0.007 \lambda_2$	$0.008 \lambda_3$
SL_2	The length of slit_2	8.0	$0.05 \lambda_1$	$0.05 \lambda_2$	$0.05 \lambda_3$
SW_2	The width of slit_2	0.9	$0.005 \lambda_1$	$0.005 \lambda_2$	$0.006 \lambda_3$
w_1	The width from left edge of patch to slit_2	34.1	$0.20 \lambda_1$	$0.22 \lambda_2$	$0.24 \lambda_3$
w_2	The width from left edge of patch to grounding strip	23.8	$0.14 \lambda_1$	$0.15 \lambda_2$	$0.17 \lambda_3$
w_3	The width of grounding strip	1.2	$0.01 \lambda_1$	$0.01 \lambda_2$	$0.01 \lambda_3$
w_4	The width from right edge of patch to grounding strip	15	$0.09 \lambda_1$	$0.10 \lambda_2$	$0.11 \lambda_3$
l_1	The length from lower edge of patch to slit_1	6.8	$0.04 \lambda_1$	$0.04 \lambda_2$	$0.05 \lambda_3$
h	Conductive ink thickness	0.01	$0.00006 \lambda_1$	$0.00006 \lambda_2$	$0.00007 \lambda_3$

radiating patch (top plate) and the ground plane, separated by a void with a distance of 8 mm. Both layers are electrically connected by a grounding strip of 1.2 mm in width. The FF antenna structure is of conductive silver ink on PET substrate and is operable at the frequency band of 1.71-2.17 GHz for 3G/4G/LTE communications. Table 1 tabulates the characteristic parameters of PET substrate and conductive silver ink. Table 2 summarizes the optimal design parameters of FF segment of the antenna at the center frequencies (1.8, 1.9, and 2.1 GHz), using CST Microwave Studio Suite.

Figures. 2(a)-(b) respectively compare the simulated $|S_{11}|$ and input impedance of conductive silver ink and perfect electric conductor (PEC) of the FF segment of the FNFC antenna. Both conductive ink and PEC achieve almost identical impedance bandwidth of 32.83% (1.68-2.34 GHz), given $|S_{11}| < -6$ dB.

Although the reflection coefficient of an antenna should be as low as possible, it is technically challenging to achieve $|S_{11}| < -10$ dB for mobile device antennas. This fact contributes to the adoption of impedance matching of less than -6 dB for integrated antennas for mobile applications [17]. Meanwhile, the real parts of input impedance of conductive

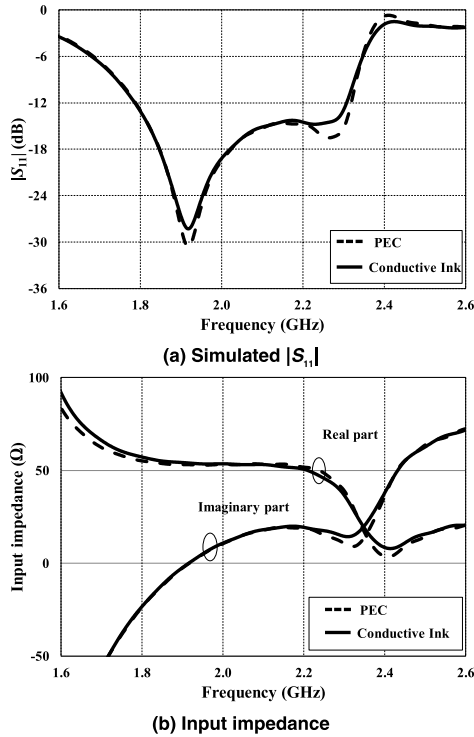


FIGURE 2. Comparison between conductive silver ink and PEC of the far-field segment.

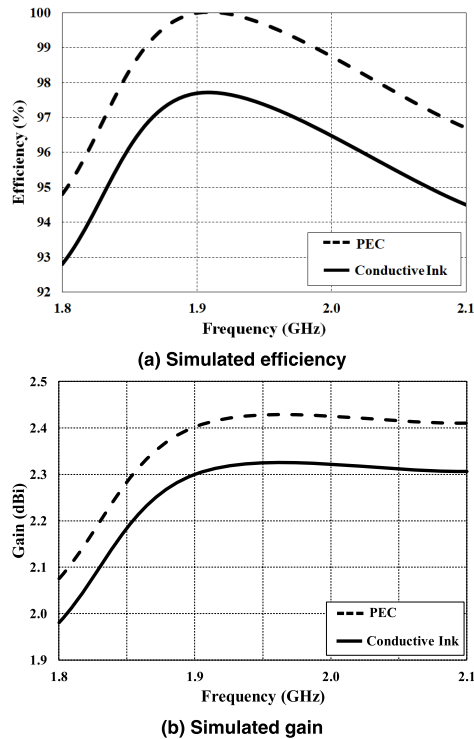


FIGURE 3. Comparison between conductive silver ink and PEC of the far-field segment.

ink and PEC vary between 50Ω and 65Ω , and the imaginary parts between -52Ω and 20Ω .

Figures 3(a)-(b) illustrate the simulated efficiency and gain of conductive silver ink and PEC of the FF segment.

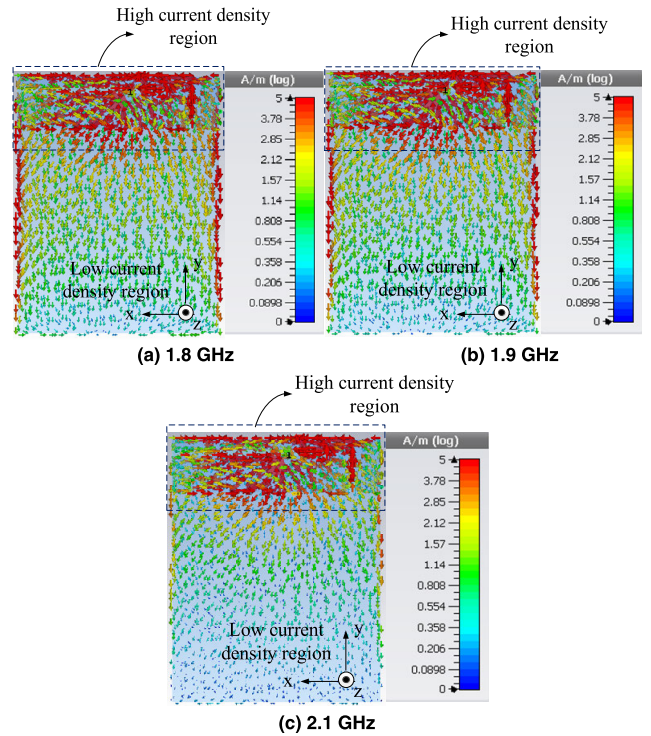


FIGURE 4. Current distribution of the far-field segment of the antenna.

At 1.8 GHz, the efficiency and gain of PEC are 95% and 2.1 dBi, and at 1.9 GHz, the efficiency is 100% with a gain of 2.4 dBi. The efficiency and gain are 97% and 2.42 dBi at 2.1 GHz. The corresponding efficiencies and gains of the FF antenna with conductive silver ink are 92%, 97%, and 94%; and 2.01 dBi, 2.3 dBi, and 2.27 dBi.

Figures 4 (a)-(c) illustrate the simulated current distribution of the far-field segment of the integrated FNFC antenna at the center frequencies of 1.8, 1.9, and 2.1 GHz. The current distribution patterns are closely similar, consisting of two distinct regions: high and low current density regions.

The high current density region was observed on the radiating patch and the upper section of the ground plane surrounding the feeding point and grounding strip. The low current density occurred on the lower section of the ground plane away from the feeding point, thus minimally affecting the radiation performance of the FF antenna. As a result, a near-field (NF) antenna for short-range communication would be integrated into the rear of the FF antenna in the low current density region (lower section of the ground plane) while the radiation performance of the FF antenna remains intact without the coupling effect.

B. THE INTEGRATED FNFC ANTENNA

Near-field communication (NFC) is a short-range wireless communication that utilizes inductive coupling technology. NFC is operable at the frequency of 13.56 MHz [23]. The advent of cashless society and changes in consumer behavior accelerate a wider adoption of electronic payment

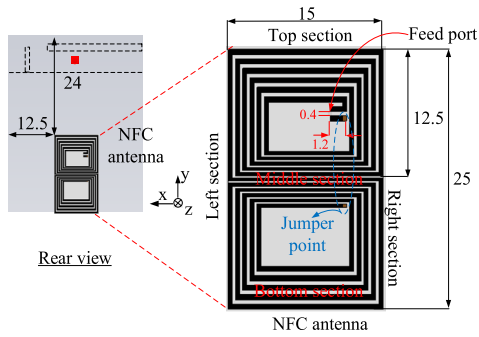


FIGURE 5. Configuration of dual-loop NFC antenna on the rear of the FF antenna (unit: mm).

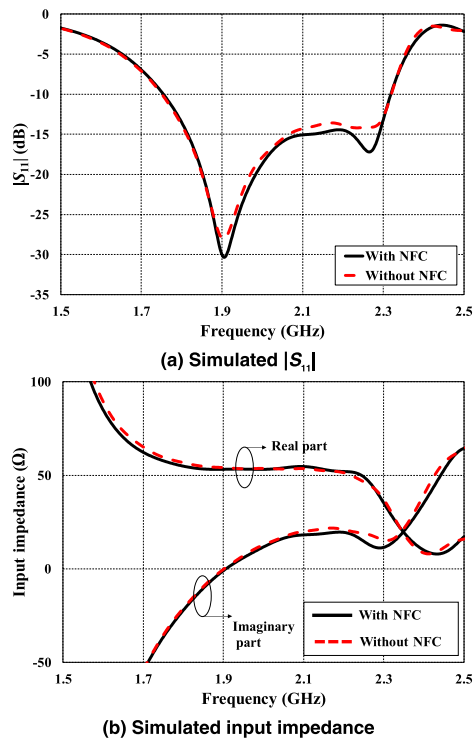


FIGURE 6. Comparison between the FF antenna with and without dual-loop NFC.

through NFC-enabled mobile devices. Besides, NFC technology plays an essential part in modern mobile payment transactions [24]–[28]. To that end, an NFC antenna for short-range communication is incorporated into modern smart devices. Thus far, a number of NFC antenna designs have been proposed [29]–[34]. In this research, a dual-loop NFC antenna [35] is mounted on the rear of the FF antenna (in the lower ground plane area), as shown in Figure 5. The NFC structure is of conductive silver ink on PET substrate.

Figures 6 (a)-(b) respectively illustrate the simulated $|S_{11}|$ and input impedance of the FF antenna in the presence and absence of dual-loop NFC. The impedance bandwidth of both antennas (32.83%, 1.68-2.34 GHz) are almost identical, given $|S_{11}| < -6$ dB. The real parts of input impedance vary between 50 Ω and 65 Ω , and the imaginary parts between -52Ω and 20 Ω . Figure 7 depicts the simulated isolation of

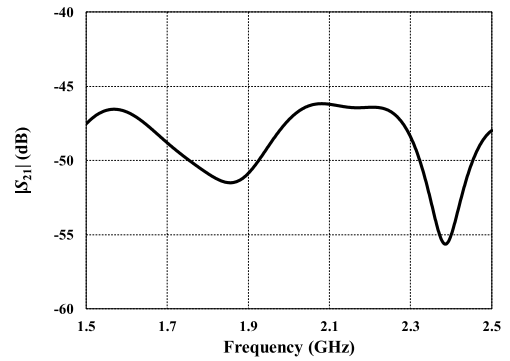


FIGURE 7. Simulated isolation $|S_{21}|$ of the integrated FNFC antenna.

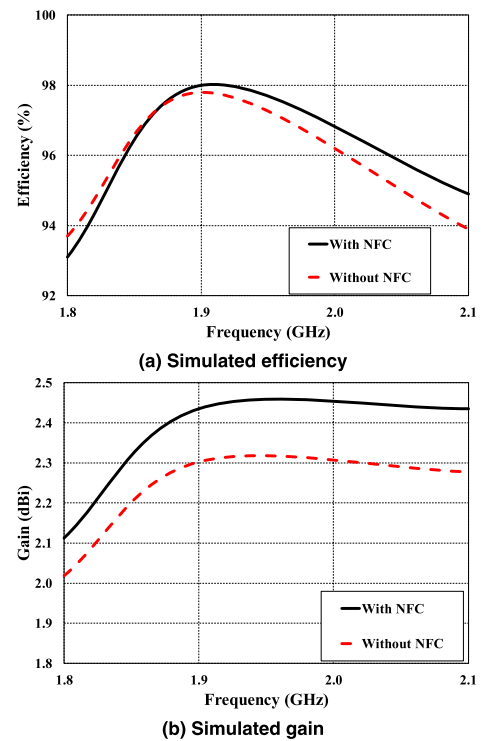


FIGURE 8. Comparison between the FF antenna with and without dual-loop NFC.

the FF antenna with dual-loop NFC in which the isolation of the FNFC antenna is below -45 dB across the target operating band (1.71-2.17 GHz).

Figures 8 (a)-(b) illustrate the simulated efficiency and gain of the FF antenna without and with dual-loop NFC. The efficiencies of the FF antenna without NFC are 94%, 98%, and 94%, with gains of 2.01, 2.3, and 2.27 dBi at the center frequencies of 1.8, 1.9, and 2.1 GHz. The corresponding efficiencies of the FF antenna with NFC are 92%, 98% and 95%, with gains of 2.06 dBi, 2.44 dBi, and 2.47 dBi.

Figures 9(a)-(d) illustrate the simulated H_x , H_y , H_z , absolute magnetic field distributions of dual-loop NFC segment of the antenna, given the frequency of 13.56 MHz. According to the right hand rule of magnetic field distribution, H_x magnetic

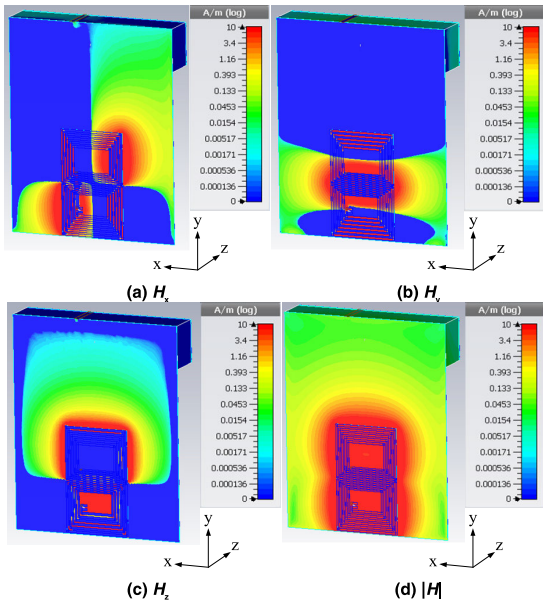


FIGURE 9. Magnetic field distribution of dual-loop NFC given the frequency of 13.56 MHz (simultaneously operated between NFC and FF antennas).

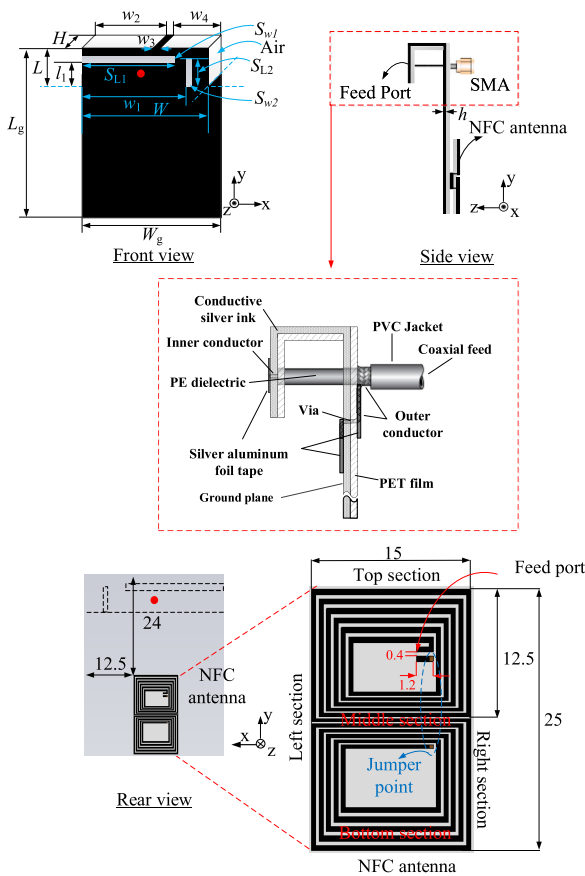


FIGURE 10. Configuration of the proposed FNFC antenna (not to scale).

field is densely distributed around the x -axis, H_y magnetic field around the y -axis, and H_z magnetic field around the z -axis. As shown in Figure 9(d), the magnetic field is distributed in all directions around the NFC antenna, and the

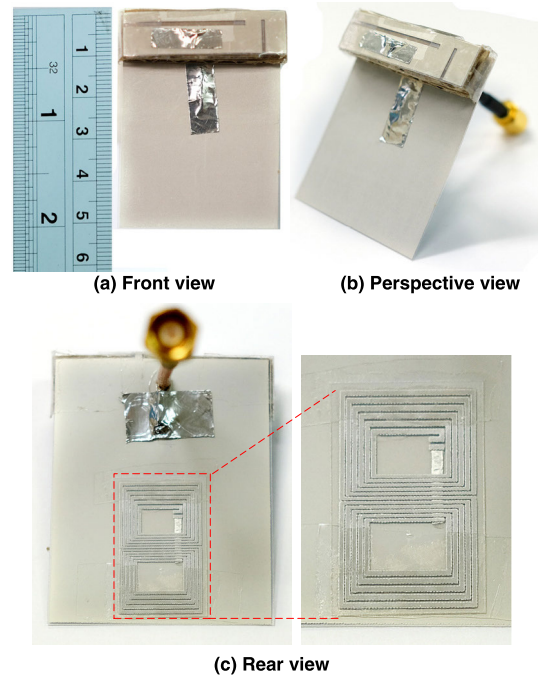


FIGURE 11. The prototype of integrated FNFC antenna.

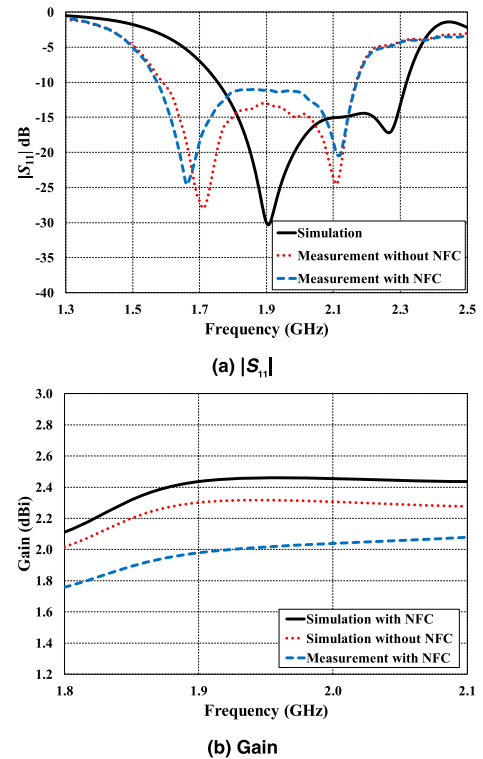


FIGURE 12. Simulated and measured $|S_{11}|$ and gains of the integrated FNFC antenna.

farther the distance the weaker the magnetic field. Ultimately, the configuration of the proposed FNFC antenna is shown in the Figure 10, and this proposed structure is used to fabricate and test to confirm the simulation results. The prototype fabrication and measured results will be discussed in the section III.

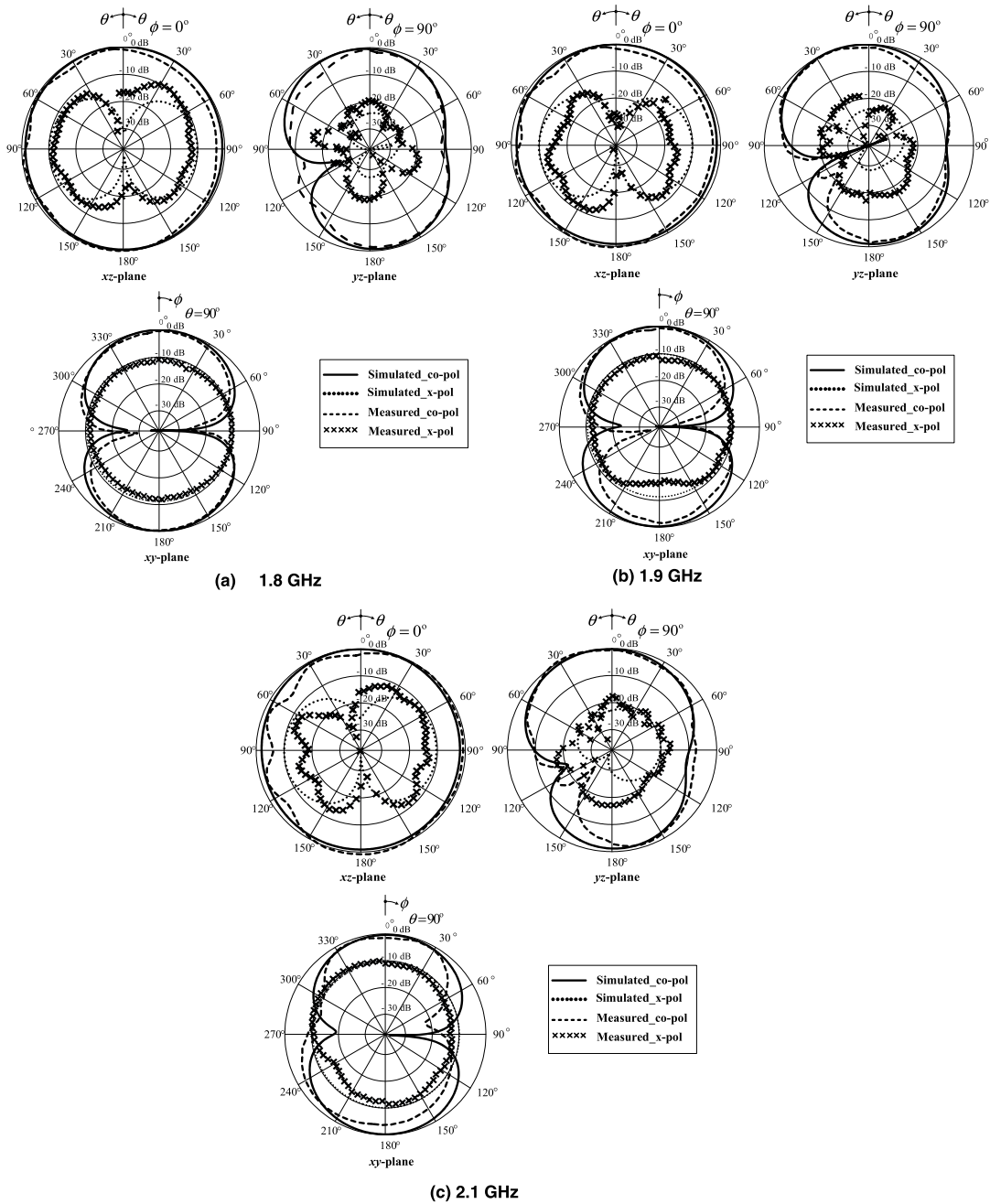


FIGURE 13. Simulated and measured radiation patterns of the integrated FNFC antenna (simultaneously operated between NFC and FF antennas).

III. PROTOTYPE FABRICATION AND MEASURED RESULTS

To validate the simulation, an antenna prototype was fabricated using screen printing method and experiments carried out. In the antenna fabrication, conductive silver ink was applied on PET substrate using a stencil of 150 meshes per inch and cured for 30 minutes at 120 °C for a conductor with 10 μm in thickness. Figure 11 depicts the prototype of the integrated FNFC antenna.

In Figure 12(a), the measured impedance bandwidth ($|S_{11}| < -6$ dB) covers the frequency range of 1.52-2.21 GHz (37%),

which is agreeable with the simulated result of 1.68-2.34 GHz (32.83%). In Figure 12(b), the minimum and maximum measured gains across the center frequencies of 1.8-2.1 GHz are 1.76-2.08 dBi, reasonably agreeable with the simulated gains of 2.06-2.47 dBi. The discrepancy could be attributed to fabrication and reflection losses.

Figures 13(a)-(c) illustrate the simulated and measured radiation patterns of the FNFC antenna at 1.8, 1.9, and 2.1 GHz, respectively. The integrated FNFC antenna achieves

TABLE 3. Measured radiation characteristics of the integrated FNFC antenna.

Characteristics	Frequency		
	1.8 GHz	1.9 GHz	2.1 GHz
HPBW (deg) in yz -plane	96	97	102
HPBW (deg) in xy -plane	92	92	92
Maximum cross-pol (dB) in xz -plane	-10	-12	-10
Maximum cross-pol (dB) in yz -plane	-15	-15	-15
Maximum cross-pol (dB) in xy -plane	-10	-10	-10
Maximum ripple (dB) in xz -plane	-3	-4	-5
Gain (dBi)	1.76	1.98	2.08

omnidirectional radiation pattern at 1.8 GHz and near-omnidirectional pattern at 1.9 GHz and 2.1 GHz due to ripples in the xz -plane. At 1.8 GHz, the radiation is of omnidirectional pattern because the maximum ripple is less than 3 dB. On the other hand, the radiation pattern is near-omnidirectional at 1.9 and 2.1 GHz as the ripples are greater than 3 dB (4 dB and 5 dB, respectively).

The polar form of radiation pattern of the FNFC antenna was characterized in xz -plane (vary θ , $\varphi = 0^\circ$), yz -plane (vary θ , $\varphi = 90^\circ$), and xy -plane (vary φ , $\theta = 90^\circ$). The simulated and measured maximum cross-polarization are approximately -10 dB for xz -, yz - and xy -planes over the target operating frequency (1.8-2.1 GHz). The simulated and measured half-power beamwidth (HPBW) in yz - and xy -planes are in the range of 90° - 100° across the operating bandwidth. The discrepancy between simulated and measured radiation patterns is caused from the imperfectness of antenna fabrication. The measured radiation characteristics of the integrated FNFC antenna are summarized in the Table 3. The FNFC antenna is suitable for 3G/4G/LTE communications despite the near-omnidirectional nature.

IV. CONCLUSION

This experimental research integrated a far-field (FF) antenna with near-field communication (NFC) antenna using PIFA structure for 3G/4G/LTE mobile devices. The integrated FNFC antenna was fabricated using conductive silver ink on polyethylene terephthalate (PET) flexible substrate. The operating frequency band of the FF segment of the antenna is 1.71-2.17 GHz, and the dual-loop NFC antenna is operable at 13.56 MHz. Simulations were carried out for optimal antenna parameters, and an antenna prototype was fabricated. The FF antenna achieved the measured impedance bandwidth of 37% (1.52-2.21 GHz), given $|S_{11}| < -6$ dB, with the minimum and maximum efficiency of 92.1% and 98%. The measured gains are 1.76-2.08 dBi across the center frequencies of 1.8-2.1 GHz with near-omnidirectional radiation pattern. The measured results are in good agreement with the simulation. The near-field segment of the antenna efficiently induces strong magnetic field distributions in H_x , H_y , and H_z orientations and is capable of communicating in the x - y - and z -axes. Essentially, the integrated FNFC antenna of conductive silver ink on PET substrate is ideal for 3G/4G/LTE applications. The measured reading performance between the NFC reader and tag antennas for mobile app will be published as future work.

REFERENCES

- [1] J. Heirons, S. Jun, A. Shastri, B. Sanz-Izquierdo, D. Bird, L. Winchester, L. Evans, and A. McClelland, "Inkjet printed GPS antenna on a 3D printed substrate using low-cost machines," in *Proc. Loughborough Antennas Propag. Conf.*, Nov. 2016, pp. 1–4.
- [2] M. Jung, J. Kim, J. Noh, N. Lim, C. Lim, G. Lee, J. Kim, H. Kang, K. Jung, A. D. Leonard, J. M. Tour, and G. Cho, "All-printed and roll-to-roll-printable 13.56-MHz-operated 1-bit RF tag on plastic foils," *IEEE Trans. Electron Devices*, vol. 57, no. 3, pp. 571–580, Mar. 2010.
- [3] A. T. Castro and S. K. Sharma, "Inkjet-printed wideband circularly polarized microstrip patch array antenna on a PET film flexible substrate material," *IEEE Antennas Wireless Propag. Lett.*, vol. 17, no. 1, pp. 176–179, Jan. 2018.
- [4] H. Liu, S. Zhu, P. Wen, X. Xiao, W. Che, and X. Guan, "Flexible CPW-fed fishtail-shaped antenna for dual-band applications," *IEEE Antennas Wireless Propag. Lett.*, vol. 13, pp. 770–773, 2014.
- [5] Q. Bai and R. Langley, "Crumpling of PIFA textile antenna," *IEEE Trans. Antennas Propag.*, vol. 60, no. 1, pp. 63–70, Jan. 2012.
- [6] L. Liu, S. Zhu, and R. Langley, "Dual-band triangular patch antenna with modified ground plane," *Electron. Lett.*, vol. 43, no. 3, pp. 140–141, Feb. 2007.
- [7] S. Nikolaou, G. E. Ponchak, J. Papapolymerou, and M. M. Tentzeris, "Conformal double exponentially tapered slot antenna (DE TSA) on LCP for UWB applications," *IEEE Trans. Antennas Propag.*, vol. 54, no. 6, pp. 1663–1669, Jun. 2006.
- [8] G. DeJean, R. Bairavasubramanian, D. Thompson, G. E. Ponchak, M. M. Tentzeris, and J. Papapolymerou, "Liquid crystal polymer (LCP): A new organic material for the development of multilayer dual-frequency/dual-polarization flexible antenna arrays," *IEEE Antennas Wireless Propag. Lett.*, vol. 4, pp. 22–26, 2005.
- [9] C.-P. Lin, C.-H. Chang, Y. T. Cheng, and C. F. Jou, "Development of a flexible SU-8/PDMS-based antenna," *IEEE Antennas Wireless Propag. Lett.*, vol. 10, pp. 1108–1111, Oct. 2011.
- [10] Z. Wang, L. Zhang, Y. Bayram, and J. L. Volakis, "Embroidered conductive fibers on polymer composite for conformal antennas," *IEEE Trans. Antennas Propag.*, vol. 60, no. 9, pp. 4141–4147, Sep. 2012.
- [11] H. R. Khaleel, H. M. Al-Rizzo, and D. G. Rucker, "Compact polyimide-based antennas for flexible displays," *J. Display Technol.*, vol. 8, no. 2, pp. 91–97, Feb. 2012.
- [12] A. Kiourti and J. L. Volakis, "Stretchable and flexible E-fiber wire antennas embedded in polymer," *IEEE Antennas Wireless Propag. Lett.*, vol. 13, pp. 1381–1384, 2014.
- [13] K. Janeczka, M. Jakubowska, G. Koziol, A. Mlozniak, and A. Arazna, "Investigation of ultra-high-frequency antennas printed with polymer pastes on flexible substrates," *IET Microw., Antennas Propag.*, vol. 6, no. 5, pp. 549–555, Apr. 2012.
- [14] A. Mehdipour, I. D. Rosca, A.-R. Sebak, C. W. Trueman, and S. V. Hoa, "Carbon nanotube composites for wideband millimeter-wave antenna applications," *IEEE Trans. Antennas Propag.*, vol. 59, no. 10, pp. 3572–3578, Oct. 2011.
- [15] H. A. E. Elobaid, S. K. A. Rahim, M. Himdi, X. Castel, and M. A. Kasegari, "A transparent and flexible polymer-fabric tissue UWB antenna for future wireless networks," *IEEE Antennas Wireless Propag. Lett.*, vol. 16, pp. 1333–1336, Dec. 2016.
- [16] Z. Hamouda, J.-L. Wojkiewicz, A. A. Pud, L. Kone, S. Bergeul, and T. Lasri, "Flexible UWB organic antenna for wearable technologies application," *IET Microw., Antennas Propag.*, vol. 12, no. 2, pp. 160–166, Jul. 2018.
- [17] Z. Zhang, *Antenna Design for Mobile Devices*, 1st ed. Hoboken, NJ, USA: Wiley, 2011.
- [18] S. Palacios, N. Ramesh, A. Rida, M. M. Tentzeris, and S. Nikolaou, "Towards an implantable wireless module with a bandwidth-enhanced antenna manufactured using inkjet-printing technology," in *Proc. IEEE Antennas Propag. Soc. Int. Symp. (APSURSI)*, Jul. 2013, pp. 2193–2194.
- [19] S. Palacios, A. Rida, S. Kim, S. Nikolaou, S. Elia, and M. M. Tentzeris, "Towards a smart wireless integrated module (SWIM) on flexible organic substrates using inkjet printing technology for wireless sensor networks," in *Proc. IEEE Int. Workshop Antenna Technol.*, Mar. 2012, pp. 20–23.
- [20] S. Palacios, S. Kim, S. Elia, A. Rida, M. M. Tentzeris, and S. Nikolaou, "Inkjet-printed planar antenna for a wireless sensor on paper operating at Wi-Fi frequency," in *Proc. IEEE Int. Symp. Antennas Propag.*, Jul. 2012, pp. 1–2.
- [21] *CST Microwave Studio Suite (User's Manual)*, CST Studio Suite (Reference Manual), Darmstadt, Germany, 2014.

[22] H. Halheit and A. V. Vorst, "A simple wideband antenna for mobile handset," in *Proc. Eur. Conf. Antennas Propag.*, Mar. 2009, pp. 553–555.

[23] J. Fischer, "NFC in cell phones: The new paradigm for an interactive world," *IEEE Commun. Mag.*, vol. 47, no. 6, pp. 22–28, Jun. 2009.

[24] H. Aziza, "NFC technology in mobile phone next-generation services," in *Proc. Int. Workshop Near Field Commun.*, Apr. 2010, pp. 21–26.

[25] S. K. Timalaina, R. Bhusal, and S. Moh, "NFC and its application to mobile payment: Overview and comparison," in *Proc. Int. Conf. Inf. Sci. Digit. Content Technol.*, vol. 1, Jun. 2012, pp. 203–206.

[26] T. Bauernfeind, P. Baumgartner, O. Bíró, A. Hackl, C. Magele, W. Renhart, and R. Torchio, "Multi-objective synthesis of NFC-transponder systems based on PEEC method," *IEEE Trans. Magn.*, vol. 54, no. 3, Mar. 2018, Art. no. 7001504.

[27] O. Sajid and M. Haddara, "NFC mobile payments: Are we ready for them?" in *Proc. SAI Comput. Conf.*, Jul. 2006, pp. 960–967.

[28] T. W. C. Brown and T. Diakos, "On the design of NFC antennas for contactless payment applications," in *Proc. Eur. Conf. Antennas Propag.*, Apr. 2011, pp. 44–47.

[29] M.-A. Chung and C.-F. Yang, "Miniaturized NFC antenna design for a tablet PC with a narrow border and metal back-cover," *IEEE Antennas Wireless Propag.*, vol. 15, pp. 1470–1474, Dec. 2015.

[30] B. Lee, B. Kim, F. J. Harackiewicz, B. Mun, and H. Lee, "NFC antenna design for low-permeability ferromagnetic material," *IEEE Antennas Wireless Propag.*, vol. 13, pp. 59–62, Jan. 2014.

[31] B. Lee, B. Kim, and S. Yang, "Enhanced loop structure of NFC antenna for mobile handset applications," *Int. J. Antennas Propag.*, vol. 2014, Apr. 2014, Art. no. 187029.

[32] W. Pachler, J. Grosinger, W. Bösch, G. Holweg, K. Popovic, A. Blümel, and E. J. W. List-Kratochvil, "A silver inkjet printed ferrite NFC antenna," in *Proc. Loughborough Antennas Propag. Conf.*, Nov. 2014, pp. 95–99.

[33] *NFC Forum*. Accessed: Oct. 8, 2019. [Online]. Available: <http://www.nfc-forum.org>

[34] *NFC Forum. NFC Analog Specification ANALOG 1.0 NFCForum-TS-Analog-1.0 2012-07-11.pdf*. Accessed: Oct. 8, 2019. [Online]. Available: <http://www.nfc-forum.org/specs/>

[35] J.-Q. Zhu, Y.-L. Ban, R.-M. Xu, C.-Y.-D. Sim, J. Guo, and Z.-F. Yu, "Miniaturized dual-loop NFC antenna with a very small slot clearance for metal-cover smartphone applications," *IEEE Trans. Antennas Propag.*, vol. 66, no. 3, pp. 1553–1558, Mar. 2018.



SITTHICHAI DENTRI (M'13) was born in Bangkok, Thailand, in February 1983. He received the B.Eng., M.Eng., and D.Eng. degrees from the Faculty of Engineering, King Mongkut's Institute of Technology Ladkrabang, Bangkok, Thailand, in 2006, 2011, and 2016, respectively. He is currently a Lecturer with the College of Industrial Technology, King Mongkut's University of Technology North Bangkok (KMUTNB).



RASSAMITUT PANSOMBOON (M'13) was born in Bangkok, Thailand, in 1987. She received the B.Eng., M.Eng., and D.Eng. degrees from the Faculty of Engineering, King Mongkut's Institute of Technology Ladkrabang (KMUTL), Bangkok, Thailand, in 2010, 2012, and 2016, respectively. She is currently working with the National Science and Technology Development Agency. She is also a member IEICE.



BANCHA LUADANG (M'16) was born in Trang, Thailand, in 1979. He received the B.Eng., M.Eng., and D.Eng. degrees from the King Mongkut's Institute of Technology Ladkrabang (KMUTL), Bangkok, Thailand, in 2003, 2011, and 2015, respectively. He is currently an Instructor with the Department of Instrumentation Engineering, Rajamangala University of Technology Ratanakosin (RMUTR). His research interests are antenna design for various mobile and wireless communications and broadcasting. He is also a member of IEICE.



ARNONG SAKONKANAPONG (S'13) was born in Nonthaburi, Thailand, in 1989. He received the B.Eng. and M.Eng. degrees from the King Mongkut's Institute of Technology Ladkrabang (KMUTL), Bangkok, Thailand, in 2011 and 2013, respectively, where he is currently pursuing the D.Eng. degree.



CHUWONG PHONGCHAROENPANICH (S'98–M'02) received the B.Eng. (Hons.), M.Eng., and D.Eng. degrees from the King Mongkut's Institute of Technology Ladkrabang (KMUTL), Bangkok, Thailand, in 1996, 1998, and 2001, respectively. He is currently an Associate Professor with the Department of Telecommunications Engineering, KMUTL, where he also serves as the Leader of the Innovative Antenna and Electromagnetic Applications Research Laboratory. His research interests are antenna design for various mobile and wireless communications, conformal antennas, and array antenna theory. He is also a member IEICE and ECTI. He serves as the Chair of the IEEE MTT/AP/ED Thailand chapter. He has been the organizing committee of several international conferences, including the TPC Chair of 2009 International Symposium on Antennas and Propagation (ISAP 2009) and a TPC member of ISAP 2012. He was on the Board Committee of ECTI Association, from 2008 to 2011 and 2014 to 2015. He was the Associate Editor of *IEICE Transactions on Communication* and the *ECTI Transactions on Electrical Engineering, Electronics, and Communications*. He is also the Associate Editor of the *IEICE ComEx*. He is also a Reviewer of many scientific journals, including *IEEE TRANSACTIONS ANTENNAS and PROPAGATION*, *IEEE ACCESS*, *IET Microwaves, Antennas and Propagation*, *Electronics Letters*, *ECTI Transactions*, and many international conferences, including ISAP and APMC.

...